Glass transition and reversible gelation in asymmetric binary mixtures: A study by mode coupling theory and molecular dynamics

Ph. Germain and S. Amokrane

Physique des Liquides et Milieux Complexes, Faculté des Sciences et Technologie, Université Paris Est (Créteil), 61 Avenue du Général de Gaulle, 94010 Créteil Cedex, France

(Received 7 May 2019; revised manuscript received 6 September 2019; published 23 October 2019)

The glass transition and the binodals of asymmetric binary mixtures are investigated from the effective fluid approach in the mode coupling theory and by molecular dynamics. Motivated by previous theoretical predictions, the hard-sphere mixture and the Asakura-Oosawa models are used to analyze experimental results from the literature, relative to polystyrene spheres mixed either with linear polymers or with dense microgel particles. In agreement with the experimental observations, the specificity of the depletant particles is shown to favor lower density gels. It further favors equilibrium gelation by reducing also the tendency of the system to phase separate. These results are confirmed by a phenomenological modification of the mode coupling theory in which the vertex functions are computed at an effective density lower than the actual one. A model effective potential in asymmetric mixtures of hard particles is used to further check this phenomenological modification against molecular dynamics simulation.

DOI: 10.1103/PhysRevE.100.042614

I. INTRODUCTION

Colloidal suspensions show a wide variety of dynamic properties and non-Newtonian behaviors. In particular, they exhibit certain nonergodic or glassy states, which do not exist in ordinary molecular or atomic fluids. In addition to the usual high-density glass associated to the steric repulsion ("caging" mechanism) one observes in certain colloidal suspensions dynamically arrested states at lower density. As they are generally associated with the existence of a short range attraction beyond the core repulsion, they are called « attractive glasses », or physical gels at low density (see, e.g., Refs. [1–8] (and [9,10] for a review). Defined in a broad way, such attractive interactions exist for example in protein suspensions [11,12], silica particles [13], polymers/colloids mixtures [3,14,15] or colloids mixed with microgel particles [8]. In such asymmetric mixtures, the effective attraction between the colloidal particles is induced by the depletion mechanism. These arrested states can have practical consequences on the thermodynamic behavior like, e.g., for protein crystallization [16], or for potential applications of their mechanical properties.

The first theoretical studies performed in the mode coupling theory (MCT [17]) adapted to colloids [18] predicted low-density gelation in hard-particles fluids with very short-range attractions [1]. Then, the question of the different scenarios for gelation stimulated vivid debates, in particular the relation between gelation and phase separation: indeed, while inducing gelation, attractive interactions also favor the fluid-fluid (F-F) transition (the crystallization can be prevented by polydispersity). Their interplay—in particular the possibility to form gels along a reversible thermodynamic path without encountering the spinodal decomposition—was therefore questioned [19] (see also [20] and refs. therein for a recent discussion). Generalizing to the glass transition the law of corresponding states [21], several authors supported the idea of a universal scenario according to which gelation would systematically occur through the spinodal decomposition, irrespective of the specificity of the attractive part of the interaction potential beyond the core [10,22,23]. This so-called "$B^{(2)}$ scenario" was based on numerical simulation results, which contradicted the pioneering work based on the MCT: the oversimplified treatment of the many-body correlations by the MCT was then invoked for explaining these discrepancies. From the experimental side, however, different behaviors were observed: while some of them seemed to corroborate the "$B^{(2)}$ scenario" [12,23–25], glass transition was also observed with no evidence of the fluid-fluid transition [15,26,27]. In Ref. [8], the role of the specificity was illustrated on two asymmetric mixtures in which hard-sphere-like polystyrene spheres are the big particles. In the first one, they were mixed with pNIPAM microgel particles and, in the second one, with linear polymers, the size ratio being kept the same in both mixtures. As a result, the use of the microgel particles as depletants tended to favor gelation in comparison with the polymer coils. In addition, microscopic phase separation was observed in the gelled samples only for the polystyrene-polymer mixtures. This confirms that specificity plays an important role for physical gelation in colloids.

Owing to a refined description of the effective potential between the colloids, we have shown in previous work [28,29] that different scenarios of colloidal gelation are possible in asymmetric binary mixtures, treated in the one-component representation. Indeed, the "$B^{(2)}$ behavior" is restricted to simple generic potentials consisting in a hard-sphere potential plus a standard short-range attraction, like in the Yukawa or the square-well potentials. This restriction, which was already pointed out by Noro and Frenkel for the binodals, is important in practice since the effective potential in real suspensions can

depart markedly from the "hard sphere + short range attraction" scheme: in mixtures of hard colloids, for example, it is oscillatory, with repulsive barriers due to the granularity of the depletant particles [30,31]. These barriers in the potential of mean force at infinite dilution, which affect also the static properties, should not be confused with the finite barriers in a free-energy landscape which are invoked to describe the dynamics beyond MCT [32]. It should indeed be recalled that the ideal MCT incorporates the interaction potential only through the static structure and ignores some dynamics processes such as activated hoping in the free energy landscape or the nonGaussian ones (see, e.g., Refs. [7,32,33] for recent work).

However, as it was shown from MCT in Refs. [28,29], these barriers in the potential of mean force at infinite dilution increase the extent of the domain in which the fluid is arrested, compared to the situation in which they are absent (see, e.g., in Ref. [29] Fig. 6 for the HS depletion potential and Fig. 8 for the square and shoulder one). In contrast, they have little influence on the equilibrium F-F binodal. Their influence on the slowing down of the dynamics was next confirmed at the level of the diffusion coefficient determined by molecular dynamics simulations [34]. Since such barriers seem to favor gelation without influencing the fluid condensation, asymmetric mixtures should generate original ways to form gels, like equilibrium gelation. its predictions about the influence of these barriers will be paralleled with those expected on physical grounds.

The first goal of this paper is to emphasize the role of the depletant in mixtures by comparing the theoretical binodals and the MCT glass transition lines to experimental data on binary mixtures [8]. Two models will be considered: the HS and the Asakura-Oosawa [35] (AO) mixtures. In the latter, a big particle interacts with another big particle or with a small one through the HS potential, but the small particles have no interaction. These models can be used as a first approximation for the two experimental situations considered PS+ microgel particles and PS+polymer, respectively, so as to analyze the role of the granularity of the depletant particles on gelation. The second goal of this work is more technical: molecular dynamics simulations are used to check the predictions from the phenomenological modification of MCT recently proposed [36,37] and aimed at improving its predictions at a quantitative level. A model closer to the physical systems analyzed here than those on which it has already been tested [36] will be used. We will compare the modified MCT glass transition line to the arrest line estimated from the behavior of the diffusion coefficient obtained from numerical simulations.

The paper is organized as follows: the theoretical framework is presented in Sec. II; Sec. III is devoted to the results and the discussion; Sec. IV is the conclusion.

II. THEORETICAL FRAMEWORK

A. EOCF representation

The results presented here are relative to asymmetric binary mixtures treated at the effective one-component fluid (EOCF) level. This well-known representation is based on the pair interaction approximation for the potential of mean force of the big particles (details are given for instance in [38–41]). The actual mixture has number densities $\rho_i = \frac{N_i}{V}$ (with N_i the number of particles of the species i and V the volume) and diameters σ_i (the corresponding volume fractions are $\eta_i = \frac{\pi}{6}\rho_i\sigma_i^3$ and the big to small particles diameter ratio is $q = \frac{\sigma_2}{\sigma_1}$). The reduction to the EOCF level is made in the semigrand ensemble (N_2, V, T, μ_1), where T the temperature and μ_1 the chemical potential of the small particles. A more convenient variable is the density ρ_1^* in the reservoir of small particles (in units of σ_1^3) as ρ_1^* is fully determined by μ_1 at fixed T. The binodals and the glass transition lines of the EOCF are then computed in the $(\rho_1^*,\ \eta_2)$ plane from the effective potential $\phi^{\text{eff}} = V_{22} + \phi^{\text{ind}}$, where V_{22} is the direct interaction potential between the big particles and ϕ^{ind} the indirect one mediated by the small particles. The latter is obtained from the pair distribution function (pdf) of the big particles g_{22} [42,43] at infinite dilution:

$$\phi^{\text{ind}}(r_{ij}) = -k_BT\{\ln(g_{22}(r, \rho_2 \to 0) - V_{22}(r)\}. \qquad (1)$$

For computing ϕ^{ind} from Eq. (1), the Ornstein Zernike equations (OZE) for the binary mixture with the big particles at infinite dilution are solved numerically with the reference hypernetted chain (RHNC) closure [44] using the bridge function computed from Rosenfeld's density functional theory [45]. The accuracy of this method for highly asymmetric mixtures has been established by comparison to simulation data [46,47]. For the Asakura-Oosawa model, the effective potential ("AO potential") has an analytical expression [36]:

$$\phi_{\text{AO}}(r) = \begin{cases} +\infty, & \frac{r}{\sigma} < 1 \\ -\frac{\pi}{4}q^3\rho_1^*\left[\frac{2}{3}\left(1+\frac{1}{q}\right)^3 - \frac{r}{\sigma}\left(1+\frac{1}{q}\right)^2 + \frac{1}{3}\left(\frac{r}{\sigma}\right)^3\right], & 1 \leqslant \frac{r}{\sigma} < 1+\frac{1}{q} \\ 0, & \frac{r}{\sigma} \geqslant 1+\frac{1}{q} \end{cases}. \qquad (2)$$

The validity of the EOCF approximation in asymmetric mixtures of hard particles has been discussed in several studies. As far as the static properties are concerned, it is quantitatively correct at large size asymmetry provided the particles do not interact through long-range interactions (more precisely, the interaction range ξ_{ij} between the particles i and j has to be comparable to $\sigma_{ij} = (\sigma_i + \sigma_j)/2$). This was established in Ref. [47] by comparison with simulations for the pdf of the big particles down to size ratios which are smaller than those investigated in this paper ($q \approx 3.33$). Furthermore, the EOCF binodals computed in several studies (e.g., refs. [38–41]) are consistent with the existing simulation data for the mixture (see Ref. [39]) and with the RHNC integral equation results for the true mixture [48]. This is naturally restricted to small particle densities $\rho_1^* < 0.8$ in the reservoir at which the small particles are in the fluid state. For the AO model, the validity

of the pair approximation is enhanced by the absence of interactions between the small particles (it is exact for $q > \frac{2}{3}\sqrt{3} - 1 \approx 6.46$ [38,49]).

The question of the EOCF is more complex for the dynamics due the presence of multiple time and length scales. A general discussion of this question is beyond the scope of this paper. Some of its aspects have been addressed in the literature from different formulations of MCT and beyond (see Refs. [7,50,51] and references therein) or the generalized self-consistent Langevin theory (GSCL; see, e.g., Ref. [52]).

We will focus here on asymmetric HS-like mixtures. For size ratios in the range $q = 5 - 10$ we consider here, some studies that treat explicitly the small and the big particles have been performed, with MCT [[36,53–55] or the GSCL approach [52]. One observes different nonergodic states in the (ρ_1, ρ_2) plane, according to the species involved in the arrest. The nonergodicity transition line shows two branches (still in the (ρ_1, ρ_2) plane): that located at low ρ_1 and large ρ_2 separates the fluid state from the so-called "depletion glass", in which only the big particle fluid is arrested (the small particle one is ergodic in the free volume let by the big ones). It is the main one at large $q(q > 5)$. The associated "depletion glass" is precisely that described in the EOCF representation. Using an accurate correspondence relation $(\rho_1, \eta_2) \to (\rho_1^*, \eta_2)$ [56], the associated density region in the semigrand ensemble is, as expected, $\rho_1^* \leqslant 0.8$ for which the small particles are in the fluid state.

The glass transition lines computed in Refs. [36,54,55], for the mixture are in qualitative agreement with those obtained here in the EOCF approximation. It was also shown in Ref. [50] for the AO model that only the EOCF representation correctly predicts the reentrant glass observed in the simulations, when the short-time mobility of the big spheres is much smaller than that of the depletant. Thus, our discussion at the EOCF level should be valid as long as the small particle fluid remains ergodic.

B. Liquid structure, binodals, and MCT arrest line

As detailed in Refs. [40,41,57] the fluid-fluid and fluid-solid binodals of the EOCF were computed from the RHNC free energy [42] using for numerical convenience the parametrized HS bridge function of Ref. [58] and a perturbation treatment for the solid [59].

For the arrest lines, the standard MCT has been used. The main steps required to determine its behavior in the long-time limit are briefly recalled here (for reviews on this well-known method see for example [17,60]). The (ideal) glassy state is characterized by the onset of a nonvanishing long-time density autocorrelation function $\langle \rho_{\mathbf{q}}(t = \infty)\rho_{-\mathbf{q}}(t = 0)\rangle$. More specifically, one computes the nonergodicity parameter $f_q = \langle \rho_{\mathbf{q}}(\infty)\rho_{-\mathbf{q}}(0)\rangle / \langle \rho_{\mathbf{q}}(0)\rho_{-\mathbf{q}}(0)\rangle$ from the following set of equations:

$$f_q = \frac{m_q}{1 + m_q}, \tag{3}$$

$$m_q = \frac{1}{2\rho} \int \frac{d\mathbf{k}}{(2\pi)^3} V(\mathbf{q}, \mathbf{k}) S_q S_k S_{q-k} f_k f_{|\mathbf{q}-\mathbf{k}|}, \tag{4}$$

$$V(\mathbf{q}, \mathbf{k}) = -\frac{1}{q^4}\left(\mathbf{q} \cdot \mathbf{k}\, \rho c_{\mathbf{k}}^{(2)} + \mathbf{q} \cdot (\mathbf{q} - \mathbf{k}) \rho c_{\mathbf{q}-\mathbf{k}}^{(2)}\right)^2. \tag{5}$$

In these equations, $c_k^{(2)}$ is the direct correlation function in reciprocal space and $S_k = \frac{1}{1-\rho c_k^{(2)}}$ the structure factor. In Eqs. (4) and (5), $m_{\mathbf{q}}$ is the memory function and $V(\mathbf{q}, \mathbf{k})$ the vertex connecting the two-point autocorrelation functions, following the factorization ansatz for the four-point correlations. The solution of Eq. (4) is then the limit of the iterative process defined by $f_q^{(0)} = 1$, $f_q^{(n+1)} = \frac{m_q(f_q^{(n)})}{1+m_q(f_q^{(n)})}$. In the MCT, the static correlation functions are the only input for studying the dynamics. This theory is known to provide a qualitatively correct description of several aspects of the glass transition. However, it oversimplifies the description of the dynamic correlations, especially close to the fluid-fluid critical point and at low density, where the dynamic heterogeneities are important [15]. It thus overestimates the extent of the glassy domain in the space of thermodynamic variables - the (ρ_1, ρ_2) plane, for example—with respect to that obtained from numerical simulations [10]. To improve the situation, different developments beyond the standard MCT have been proposed, starting from the exact time evolution equation [60–63]. They attempt to better treat the many-body correlations either by nonperturbative approaches (see Ref. [59] for a review) or beyond the factorization ansatz [61–63]. Other lines of attack developped by Schweizer and coworker incorporate the hopping processes [7,32], and extend the local cage approach in the nonlinear Langevin equation to include collective effects (see references in Ref. [33]). For a review of alternative approaches see, for example, Ref. [64].

Besides these theoretical developments, phenomenological approaches consist in using effective parameters in the framework of the traditional MCT (see, for example, Refs. [65–67]). In Refs. [35,36] a simple means was proposed to reduce the too-strong memory effect resulting from the factorization ansatz and thus offset the tendency of MCT to systematically overestimate the magnitude of the dynamic correlations: The static input in the vertex should be computed for an effective density lower than the actual one (and hence the designation of density-retarded vertex in Ref. [36]), thus at a state point corresponding to a less correlated fluid. This modification was calibrated from the one component HS fluid: $\eta_{\text{eff}} = \eta - \Delta\eta$ with $\Delta\eta = \eta_g^{\text{ex}} - \eta_g^{\text{MCT}}$. Thus, $\Delta\eta$ is the difference between the « exact » critical glass packing fraction (more precisely, the experimental one for HS-like colloids) and the MCT one. With $\eta_g^{\text{ex}} = 0.58$ and $\eta_g^{\text{MCT}} = 0.525$, one gets $\Delta\eta = 0.055$ (the modification appropriate for model potential which depart much from HS ones will be discussed in Sec. III). In spite of its purely phenomenological character, this ansatz improves significantly the accuracy of MCT with respect to the numerical simulation data for hard particle fluids and some with soft interactions [35]: This was shown for the glass transition lines, but also the α-relaxation close to the arrest transition and for several rheological properties [36]. Thus, in parallel to the theoretical improvements of MCT based on a microscopic analysis, this "modified" version (hereafter referred to as MMCT) proves useful from a practical point of view.

C. Molecular dynamics

For the purpose of checking the MCT predictions in the particular situations investigated here, we used molecular

dynamics for estimating the arrest line from the behavior of the diffusion coefficient D:

$$D = \lim_{t\to\infty} \frac{\langle \mathbf{r}(t)^2 \rangle}{6t}, \tag{6}$$

where the numerator is the average mean square displacement computed by integrating the contributions of all the particles for different initial times. A simulation box with $N = 8^3$ or 10^3 particles was used. The equation of motion was integrated with the standard Verlet algorithm using a reduced time step $\Delta t = 2.10^{-4}$ (corresponding to a displacement $\Delta r \sim 10^{-4} \times \sigma$). Distances were measured in units of the diameter σ, the simulation time in units of $t_0 = \sigma \times (m/k_BT)^{1/2}$ and diffusion coefficients in units of $D_0 = \sigma^2/t_0 =$, where m is the particle mass and T the temperature. The Andersen thermostat was used for reaching equilibrium after about 1.510^6 time steps; then D was determined in the micro-canonical ensemble, still over 1.510^6 time steps. This method was validated by comparison with results from the literature obtained for standard potentials and the pdf was compared with the RHNC one to check for the possibility of being in a two-phase domain not seen in the finite size simulation (details are given in Ref. [34]).

III. RESULTS AND DISCUSSION

A. Binodals and glass transition lines of asymmetric mixtures: Effect of the specificity

In a previous paper, we investigated the equilibrium and the glass transition lines of the HS mixture and of the Asakura-Oosawa one in the EOCF representation [57]. The results underlined the influence of the size ratio but also that of the granularity of the small particles, which is incorporated in the HS mixture model but not in the AO one as mentioned above. Comparing these theoretical predictions with experimental results should be made with care. However, the two mixtures investigated in Ref. [8]—the microgel—polystyrene colloid mixture and the polymer/polystyrene one—provide an interesting experimental reference: Indeed, while in both of them, the big polystyrene spheres can be considered as hard spherelike ones, the small-small interactions strongly differ in the two models. Due to their dense brushlike outer layers, the pNIPAM microgel particles in the first mixture also have a hard-sphere-like behavior. On the contrary, the polymer-polymer interactions in the second one are often neglected in the literature due to the dispersed nature of the polymer coils (the AO mixture model should thus be appropriate). Though the correspondence between the models and the real suspension is certainly not strict, comparing the experimental behavior of these two mixtures with those predicted for the AO and the HS mixture models should be instructive.

Experimentally, gelation is observed in both mixtures inside a large F-S coexistence domain that widens for similar packing fractions: $\eta_1 \leqslant 0.2$. However, gels are observed at lower packing fraction in the microgel–polystyrene mixture than in the polymer/polystyrene one: they indeed exist down to $\eta_2 = 0.04$ in the former (Fig. 2) and only for $\eta_2 > 0.25$ in the latter. Furthermore, microscopic heterogeneities are observed in the gelled samples for the polymer/polystyrene mixture (such observations are not reported for the microgel—polystyrene one although the question of the vicinity of the F-F transition is discussed on theoretical grounds).

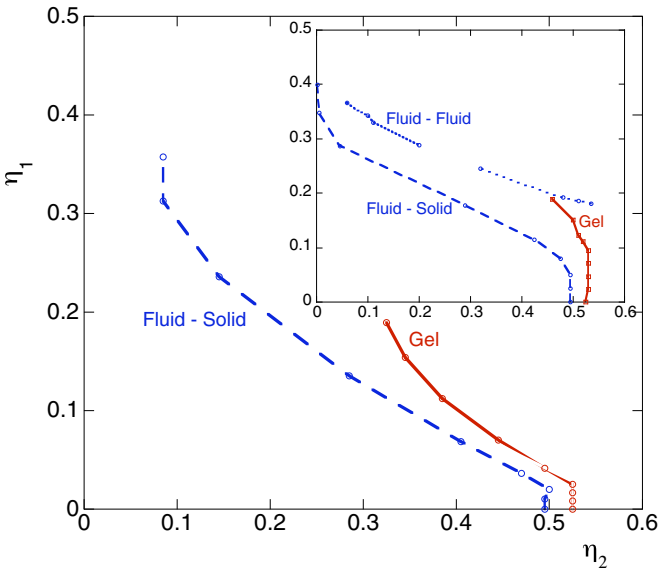

FIG. 1. Crystallization and glass transition line for the HS and AO (inset) mixtures for $q = 5$.

For analyzing these results, we computed the binodals and the glass transition line of the AO and the HS mixture models in the (ρ_1, η_2) plane. They were first computed for the EOCF in the (ρ_1^*, η_2) plane. Next, ρ_1 was deduced from ρ_1^* and η_2 by the accurate expression derived in Ref. [56] for the HS mixture and from the relation $\rho_1 = \rho_1^*(1 - \rho_2 \frac{\pi(\sigma_1+\sigma_2)^3}{6})$ for the AO one [57]. The latter, in which the factor $1 - \rho_2 \frac{\pi(\sigma_1+\sigma_2)^3}{6} = 1 - \eta_2(1 + \frac{1}{q})^3$ is the free volume fraction let by the big particles in the mixture, is also accurate for large q. The results are shown in Figs. 1–3 for $q = 5$,8, and 10. First, the glass transition line is systematically located within the F-S coexistence (Figs. 1 and 2). However, the arrested

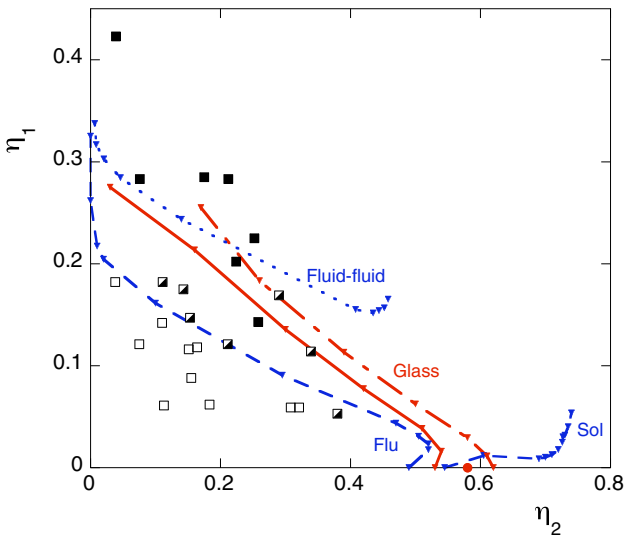

FIG. 2. Binodals and glass transition lines for the HS mixture with $q = 10$.

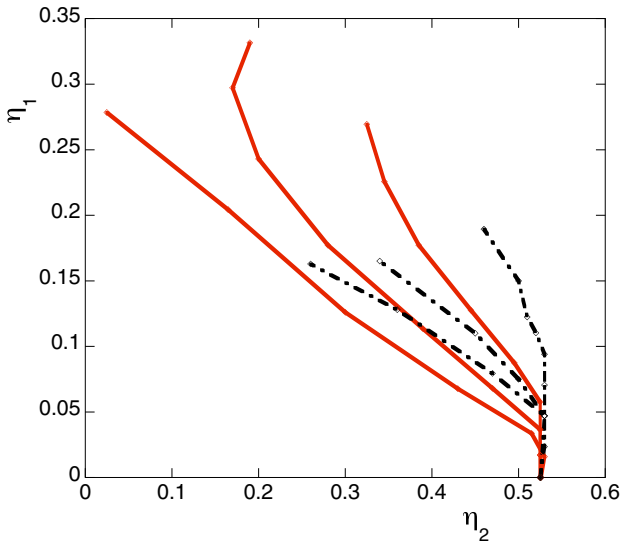

FIG. 3. MCT glass transition lines of the HS mixture (solid line) and for the AO mixture (dashed line) for $q = 5$, 8, and 10, from right to left.

state domain widens with q and is more extended for the HS mixture model than for the AO one (Fig. 3). Furthermore, the F-F transition line exists systematically in the AO mixture, while it is observed only for $q = 10$ in the HS mixture (the critical ratio q_c for which the F-F line disappears for this model lies in the range $8 < q_c < 9$). Therefore, a correlation exists between the experimental results and the theoretical predictions. This concerns especially the extent of the domain on the nonergodic states and, in a more hypothetic way, the F-F condensation. The fact that low-density gels are more likely in the HS mixture than in the AO one is due to two factors:

(i) The specific behavior of the HS depletion potential: It is oscillatory and presents repulsive barriers whose height and width increase with the density of small particle. The main barrier located just beyond the depletion well contributes to stabilizing the "bonds" induced by this depletion attraction between particles close to contact (see Ref. [34] for a discussion from MD simulation). This favors the dynamical arrest.

(ii) The F-F transition systematically competes gelation in the AO mixture model, while for the HS one, it does not exist for $q = 5$, 8. For $q = 10$, the F-F line exists but it is preempted by the glass transition line over a wide domain of density. Thus, in the AO mixture, the ergodic-nonergodic transition is found at larger packing fractions of the big particles than in the HS one.

In Fig. 2 the theoretical binodals and the glass transition line of the HS mixture with $q = 10$ are compared with that of the microgel—polystyrene mixture. The agreement already underlined in Ref. [8] for the F-S transition line is also good for the nonergodic states. This is confirmed by MMCT, shown to be accurate for the HS model [36].

Concerning the F-F transition, the possible existence of a metastable « hidden » F-F transition was discussed in Ref. [8], although no clear signs of phase separation were reported. One should note that the experimental size ratio $q \simeq 9.1$ is close to the theoretical limiting size ratio for the appearance of the F-F transition in the HS mixture. As discussed by the authors, the precise determination of the particle diameters is a difficult task, especially for the microgel ones. Furthermore, previous studies have shown that the presence of « residual » interactions in HS mixtures (like those probably existing between the brush-like outer layers) can suppress the F-F binodal [68].

Solid curve: MCT glass transition line; Long-dash short-dashed curve: same for MMCT. Squares: experimental points from [8] (microgel/polystyrene mixture for $q = 0.11$); empty squares: homogeneous fluid; half-filled squares: fluid-solid coexistence; filled squares: gel. The computed fluid-solid and fluid-fluid binodals are shown by the dashed line. The filled circle on the abscissa axis shows the critical value for HS colloids

The experimental results are thus consistent with the theoretical predictions. Both confirm the role of the specificity in the behavior of colloidal suspensions, in particular the scenario for gelation, which is not universal. This contrasts with the view resulting from "simple," generic interaction potentials consisting in a hard core + short-range attraction. It is observed here for asymmetric mixtures with different depletant particles.

B. Assessing MCT for the effective potential in asymmetric mixtures of hard-sphere-like colloids

In this section molecular dynamics simulations are used to check the predictions from MCT and the modified version, for asymmetric mixtures. A "toy potential" is used in which the indirect part is that of the HS mixture with $q = 5$. This value is motivated by the fact that equilibrium gelation is more likely at this size ratio since the F-F binodal is either absent or moved to higher depletant packing fractions. Since we did not use a simulation code specialized for the HS potential, a power-law form was used for the direct potential V_{22}:

$$V_{22}(r) = \epsilon \left(\frac{\sigma}{r}\right)^{32}. \tag{7}$$

Figure 4 shows the effect of ρ_1^* on the depth of the depletion well and on the height of the repulsive barrier. Accordingly, increasing ρ_1^* is expected to favor gelation.

We have then compared the MCT glass transition line obtained for this potential to an arrest line estimated from the behavior of the diffusion coefficient determined by molecular dynamics. The results were computed for the reduced temperature $T^* = \frac{k_B T}{\epsilon}$. Concerning the simulation dynamics, the system was homogenous in all the situations considered. However, when approaching the arrested state $D(t) = \frac{\langle \mathbf{r}(t)^2 \rangle}{6t}$ hardly stabilizes during the simulation time (this is why a large simulation time was used). For high ρ_1^*, the temperature was difficult to stabilize up to the end of the 1.5×10^6 time steps. This can be understood as the consequence of the structuration of the effective potential, especially the large potential barrier which traps the particles pairs close to contact (see, e.g., Fig. 6).

This effect was analyzed in Ref. [34] where different lifetimes of the pair bonds were computed for similar potentials. The typical value of the bond lifetime is $\tau \sim 10^5 \Delta t$

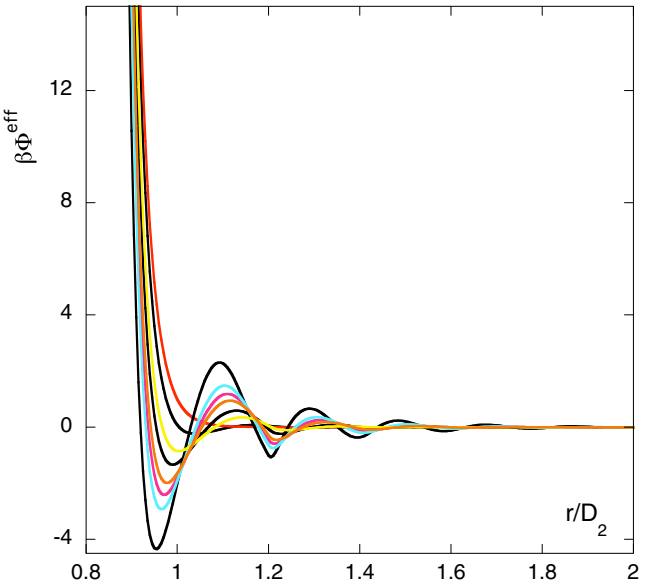

FIG. 4. Effective potential for a HS mixture with $q = 5$ and $\rho_1^* = 0,\ 0.2,\ 0.4,\ 0.6,\ 0.65,\ 0.7, 0.8$ (from top to bottom).

in this density region. As τ is not so small with respect to the simulation time, the kinetic energy hardly stabilized during the simulation. On account of these difficulties we could determine $(D(\rho_2))$ down to $10^{-4}D_0$, in the range $\rho_1^* \leqslant 0.7$. The iso $-D(\rho_1^*, \rho_2) = 10^{-4}D_0$ line was thus chosen for correlating the MD to the MCT ideal glass transition line. An example of its construction is shown in Fig. 5 for $\rho_1^*\sigma_1^3 = 0.6$, $D = 10^{-4}D_0$ is found for $1.30 \leqslant \rho_2\ \sigma_2^3 \leqslant 1.31$. This shows that the line $D(\rho_1^*, \rho_2) = 10^{-4}D_0$ could be determined with sufficient resolution in the corresponding value of ρ_2.

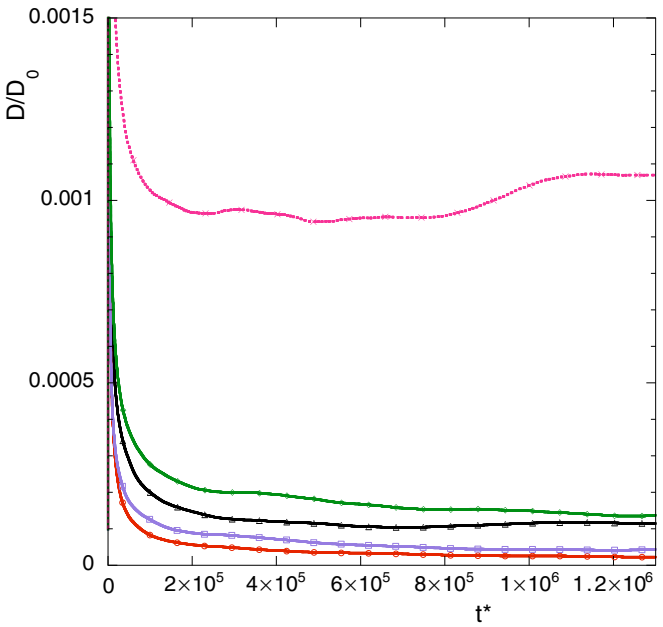

FIG. 5. $D(t^*)$ computed for the effective potential in a HS mixture with $q = 5$ and $\rho_1^*\sigma_1^3 = 0.6$. The big spheres density is $\rho_2\sigma_2^3 = 1.25,\ 1.29,\ 1.30,\ 1.31, 1.32$ from top to bottom.

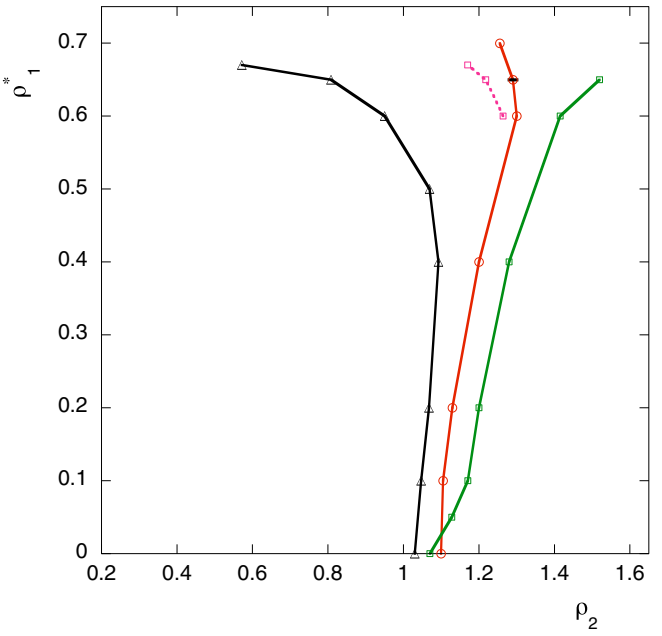

FIG. 6. MCT nonergodicity lines and MD isodiffusivity line for the binary mixture with pure HS potential V_{12}. Triangles: original MCT; squares: modified MCT. The three points on the dotted line have been obtained with the $(\Delta\eta_{\rm HS}, \rho_1^{*\rm eff})$ correction, as explained in the text. Circles: iso-diffusivity line from the MD simulation (an error bar is shown for $\rho_1{}^* = 0.65$).

The comparison with the original and modified MCT is shown in Fig. 6. Both lines actually signal an important slowing down in the dynamics but it is stressed that it is characterized differently in these methods: the MCT line corresponds to the onset of a nonvanishing value of the long time of the density autocorrelation function, while the simulation one is actually a line of very low diffusivity (see, for example, Refs. [60,64,69] and references therein for the nonexistence of the sharp transition predicted by MCT). In practice, the correlation between both lines can be judged here in Fig. 6, from the rapid variation of the diffusion coefficient in a narrow density range around the "zero" diffusivity line. This question, as well as the lowest diffusion coefficient that can be achieved in simulation (see also Ref. [70] for a similar procedure) or in real experiments will thus not be discussed further here as this would require very extensive simulations and experiments.

One first observation is that the re-entrance of the glassy state predicted by the original MCT is confirmed by the MD simulation. It is, however, exaggerated quantitatively. This is likely related to the fact that with $\phi^{\rm eff}(r)$ the arrest is now not exclusively related to the repulsion. One important feature of $\phi^{\rm eff}(r)$ is indeed its dependence on ρ_1^* which plays a role similar to an inverse temperature, as discussed in Ref. [36] for the Lennard-Jones or the square-well models. This dependence becomes crucial at low density when one enters the regime of the attractive glass or the gel. For determining this line with the modified version, the two regimes cannot be thus treated with the pure HS correction. In the regime of the repulsive glass, the simplest extension of the correction for hard spheres is $\Delta\eta = (\frac{0.58}{d_{\rm HS}^3} - \eta_{\rm MCT}^g)$ as for the Lennard-Jones potential [36].

One needs then to specify an effective HS diameter ^{d}HS. This is however not immediate for the oscillatory effective potentials $\phi(r)$. Here, ^{d}HS was taken as the HS diameter that gives the same second virial coefficient as the WCA part [43] of $\phi^{\text{eff}}(r)$.

The arrest line computed in this way is slightly shifted with respect to the isodiffusivity line but the trend is the same up to $\rho_1^* \approx 0.6$. In the regime of the attractive glass and in the gel, the above correction *should not* be used actually. Indeed, due to the attractions, the uncorrected value η^g_{MCT} decreases significantly when $\rho_1{}^*$ increases. $\Delta\eta$ becomes eventually comparable to the uncorrected value, a sign that the HS-like recipe for the "correction" is incorrect, understandably. There is however no simple way to incorporate this role of attractions, but a heuristic one is to compute $\phi^{\text{eff}}(r)$ at an effective value $\rho_1^{*,\text{eff}}$ that takes into account the modified density of the big spheres. The expected value $\rho_1^{*,\text{eff}} < \rho_1^*$ would result in a decrease of the strength of $\phi^{\text{eff}}(r)$. We thus tentatively combined—in the region of the reentrance—a pure HS correction $\Delta\eta_{\text{HS}} = 0.55/d^3_{\text{HS}}$ with $\phi^{\text{eff}}(r)$ computed at an effective packing fraction $\rho_1^{*,\text{eff}}$ estimated from the scaled-particle theory [43]. The overall effect of this combined $(\Delta\eta_{\text{HS}}, \rho_1^{*,\text{eff}})$ correction is to bring the MCT line closer to that estimated by simulation. Furthermore, a smooth transition between the two regimes—HS-like and combined correction—needs to be established. The surprising agreement observed in Fig. 6 asks, however, for further investigation. It might well be that these *ad hoc* shifts of the densities invoked to reduce the memory effect account empirically for the physical mechanisms such as the hopping processes that lack in MCT.

IV. CONCLUSIONS

In this paper, we first investigated the effect of the depletant particles on the glass transition lines and the binodals in asymmetric mixtures of hard-sphere-like colloids. Two theoretical models, the AO and the HS mixture ones, were considered for describing hard colloidal particles mixed on the one hand with weakly interacting polymers coils, and with hard particles on the other hand. Using the EOCF representation of the mixture, the binodals were computed from accurate liquid state methods and the line of dynamical arrest from the mode coupling theory.

The comparison with experiments on two mixtures of hard polystyrene spheres mixed either with dense microgel particles or with polymer coils, with the same size ratio, showed a fair agreement for the binodals but also for the glass transition lines. The different behaviors with the two depletant particles can be understood from the specificities of the potential of mean-force at infinite dilution. Indeed, contrarily to the AO model in which it is purely attractive beyond the core, the so-called HS depletion potential has an oscillatory behavior, with attractive parts and repulsive barriers. We showed that this favors lower density gelation consistently with experiment. On the other hand, that this difference at the level of the transition lines can be accounted for in the framework of MCT is rather unexpected since the interactions are involved in MCT only through the input static structure.

Last, besides the comparison with experiment, the simple, phenomenological modification of MCT recently proposed, was checked versus simulation on a model potential appropriate to this situation. While confirming the qualitative trends deduced from the original MCT, the modification improves significantly the quantitative agreement with simulation, although this requires and *ad hoc* extension with respect to the one-component fluid so as to cope for the presence of the depletants. Its generalization for incorporating the dependence of the effective interaction potential in hard-sphere-like colloids on the physical parameters such as the depletant density or the temperature should stimulate further work for a quantitative use of MCT for the study of mixtures of practical interest.

[1] J. Bergenholtz and M. Fuchs, Phys. Rev. E **59**, 5706 (1999); J. Phys. Condens. Matter **11**, 10171 (1999).

[2] K. A. Dawson, G Foffi, F. Sciortino, P. Tartaglia, and E. Zaccarelli, J. Phys.: Condens. Matter **13**, 9113 (2001).

[3] Pham *et al.*, Science **296**, 104 (2002); K. H. Pham, S. U. Egelhaaf, P. N. Pusey, and W. C. K. Poon, Phys. Rev. E **69**, 011503 (2004).

[4] G. Foffi, K. A. Dawson, S. V. Buldyrev, F. Sciortino, E. Zaccarelli, and P. Tartaglia, Phys. Rev. E **65**, 050802(R) (2002).

[5] A. M. Puertas, M. Fuchs, and M. E. Cates, Phys. Rev. Lett. **88**, 098301 (2002); Phys. Rev. E **67**, 031406 (2003).

[6] E. Zaccarelli, F. Sciortino, and P. Tartaglia, J. Phys.: Condens. Matter **16**, S4849 (2004).

[7] Y. L. Chen and K. S. Schweizer, J. Chem. Phys. **120**, 7212 (2004); D. C. Viehman and K. S. Schweizer, *ibid.* **128**, 084509 (2008).

[8] K. Bayliss, J. S. van Duijneveldt, M. A. Faers, and A. W. P. Vermeer, Soft Matter **7**, 10345 (2011).

[9] K. Dawson, Curr. Opin. Colloid Interface Sci. **7**, 218 (2002).

[10] E. Zaccarelli, J. Phys.: Condens. Matter **19**, 323101 (2007).

[11] N. M. Dixit and C. F. Zukoski, Phys. Rev. E **67**, 061501 (2003).

[12] F. Cardinaux, T. Gibaud, A. Stradner, and P. Schurtenberger, Phys. Rev. Lett. **99**, 118301 (2007).

[13] M. C. Grant and W. B. Russel, Phys. Rev. E **47**, 2606 (1993).

[14] T. Eckert and E. Bartsch, Phys. Rev. Lett. **89**, 125701 (2002).

[15] J. Bergenholtz, W. C. K. Poon, and M. Fuchs, Langmuir **19**, 4493 (2003).

[16] G. Foffi, G. D. McCullagh, A. Lawlor, E. Zaccarelli, K. A. Dawson, F. Sciortino, P. Tartaglia, D. Pini, and G. Stell, Phys. Rev. E **65**, 031407 (2002).

[17] W. Götze, in *Liquids, Freezing, and Glass Transition*, edited by J.-P. Hansen, D. Levesque, and J. Zinn-Justin (North-Holland, Amsterdam, 1991), p. 287.

[18] G. Szamel and H. Löwen, Phys. Rev. A **44**, 8215 (1991).

[19] G. Foffi, C. De Michele, F. Sciortino, and P. Tartaglia, Phys. Rev. Lett. **94**, 078301 (2005); J. Chem. Phys. **122**, 224903 (2005).

[20] C. P. Royall, S. R. Williams, and H. Tanaka, J. Chem. Phys. **148**, 044501 (2018).

[21] M. G. Noro and D. Frenkel, J. Chem. Phys. **113**, 2941 (2000).
[22] F. Sciortino, Eur. Phys. J. B **64**, 505 (2008).
[23] P. J. Lu, E. Zaccarelli, F. Ciulla, A. B. Schofield, F. Sciortino, and D. A. Weitz, Nature **453**, 499 (2008).
[24] E. Zaccarelli, P. J. Lu, F. Ciulla, D. A. Weitz, and F. Sciortino, J. Phys.: Condens. Matter **20**, 494242 (2008).
[25] B. Ruzicka, L. Zulian, R. Angelini, M. Sztucki, A. Moussaïd, and G. Ruocco, Phys. Rev. E **77**, 020402(R) (2008).
[26] S. Ramakrishnan, M. Fuchs, K. S. Schweizer, and C. F. Zukoski, J. Chem. Phys. **116**, 2201 (2002).
[27] S. A. Shah, Y.-L. Chen, K. S. Schweizer, and F. C. Zukoski, J. Chem. Phys. **119**, 8747 (2003).
[28] Ph. Germain and S. Amokrane, Phys. Rev. Lett. **102**, 058301 (2009).
[29] Ph. Germain and S. Amokrane, Phys. Rev. E **81**, 011407 (2010).
[30] B. Gotzelmann, R. Evans, and S. Dietrich, Phys. Rev. E **57**, 6785 (1998).
[31] S. Amokrane and J.-G. Malherbe, J. Phys.: Condens. Matter **13**, 7199 (2001); **14**, 3845(E) (2002).
[32] K. S. Schweizer and E. J. Saltzman, J. Chem. Phys. **119**, 1181 (2003).
[33] R. Zhang and K. Schweizer, J. Phys. Chem. B **122**, 3465 (2018).
[34] E. Ndong Mintsa, Ph. Germain, and S. Amokrane, Eur. Phys. J. E **38**, 21 (2015).
[35] S. Asakura and F. Oosawa, J. Chem. Phys. **22**, 1255 (1954); J. Polym. Sci. **33**, 183 (1958).
[36] S. Amokrane, F. Tchangnwa Nya, and J. M. Ndjaka, Eur. Phys. J. E **40**, 17 (2017).
[37] S. Amokrane and Ph. Germain, Phys. Rev. E **99**, 052120 (2019).
[38] N. G. Almarza and E. Enciso, Phys. Rev. E **59**, 4426 (1999).
[39] M. Dijkstra, R. van Roij, and R. Evans, Phys. Rev. Lett. **81**, 2268 (1998); **82**, 117 (1999); Phys. Rev. E **59**, 5744 (1999).
[40] J. Clement-Cottuz, S. Amokrane, and C. Regnaut, Phys. Rev. E **61**, 1692 (2000).
[41] J. G. Malherbe, C. Regnaut, and S. Amokrane, Phys. Rev. E **66**, 061404 (2002).
[42] T. L. Hill, *Statistical Mechanics* (Dover publications, New York, 1987).
[43] J. P. Hansen and I. R. Mc Donald, *Theory of Simple Liquids* (Academic Press, San Diego, 2005).
[44] F. Lado, S. M. Foiles, and N. W. Ashcroft, Phys. Rev. A **28**, 2374 (1983).
[45] Y. Rosenfeld, J. Chem. Phys. **98**, 8126 (1993).
[46] H. Shinto, M. Miyahara, and K. Higashitani, J. Colloid Interface Sci. **209**, 79 (1999).
[47] J.-G. Malherbe and S. Amokrane, Mol. Phys. **99**, 335 (2001); S. Amokrane, A. Ayadim, and J. G. Malherbe, J. Phys.: Condens. Matter **15**, S3443 (2003).
[48] A. Ayadim and S. Amokrane, Phys. Rev. E **74**, 021106 (2006).
[49] M. Dijkstra, J. M. Brader, and R. Evans, J. Phys.: Condens. Matter **11**, 10079 (1999).
[50] E. Zaccarelli, H. Löwen, P. P. F. Wessels, F. Sciortino, P. Tartaglia, and C. N. Likos, Phys. Rev. Lett. **92**, 225703 (2004).
[51] M. Priya, N. Bidhoodi, and S. P. Das, Phys. Rev. E **92**, 062308 (2015); N. Bidhoodi and S. P. Das, *ibid.* **92**, 062309 (2015).
[52] R. Juárez-Maldonado and M. Medina-Noyola, Phys. Rev. E **77**, 051503 (2008).
[53] G. Nägele, J. Bergenholtz, and J. K. G. Dhont, J. Chem. Phys. **110**, 7037 (1999).
[54] T. Voigmann, Euro Phys. Lett. **96**, 36006 (2011).
[55] F. Tchangnwa Nya, A. Ayadim, Ph. Germain, and S. Amokrane, J. Phys.: Condens. Matter **24**, 325106 (2012).
[56] R. Roth, R. Evans, and A. A. Louis, Phys. Rev. E **64**, 051202 (2001).
[57] Ph. Germain and S. Amokrane, Phys. Rev. E **76**, 031401 (2007).
[58] A. Malijevsky and S. Labik, Mol. Phys. **60**, 663 (1987); S. Labik and A. Malijevski, *ibid.* **67**, 431 (1989).
[59] M. Hasegawa, J. Chem. Phys. **108**, 208 (1998).
[60] S. P. Das, Rev. Mod. Phys. **76**, 785 (2004).
[61] G. Szamel, Phys. Rev. Lett. **90**, 228301 (2003).
[62] J. Wu and J. Cao, Phys. Rev. Lett. **95**, 078301 (2005).
[63] L. M. C. Janssen and D. R. Reichman, Phys. Rev. Lett. **115**, 205701 (2015).
[64] L. Berthier and G. Biroli, Rev. Mod. Phys. **83**, 587 (2011).
[65] Th. Voigtmann, A. M. Puertas, and M. Fuchs, Phys. Rev. E **70**, 061506 (2004).
[66] A. J. Banchio, J. Bergenholtz, and G. Nagele, Phys. Rev. Lett. **82**, 1792 (1999).
[67] F. Sciortino, P. Tartaglia, and E. Zaccarelli, Phys. Rev. Lett. **91**, 268301 (2003).
[68] Ph. Germain, J. G. Malherbe, and S. Amokrane, Phys. Rev. E **70**, 041409 (2004); Ph. Germain, J. Chem. Phys. **133**, 044905 (2010).
[69] W. Kob, S. Roldan-Vargas, and L. Berthier, Phys. Procedia **34**, 70 (2012).
[70] E. Zaccarelli, G. Foffi, K. A. Dawson, S. V. Buldyrev, F. Sciortino, and P. Tartaglia, Phys. Rev. E **66**, 041402 (2002).